Summary: In the present investigation we have developed a novel technique to synthesize nanocomposite materials consisting of SC-15 epoxy resin and silicon carbide (β-SiC) nanoparticles. A high intensity ultrasonic liquid processor was used to obtain a homogeneous molecular mixture of epoxy resin and β-SiC nanoparticles. In this study, we have prepared three different samples containing 0.5, 1, and 1.5% of β-SiC nanoparticles by weight of the epoxy resin. In parallel, control samples were also made following identical procedures without the infusion of nanoparticles. Test samples were characterized by TGA, DSC and three-point bend flexural tests to evaluate thermal and mechanical properties. The results indicate that 1 wt.-% loading derives the maximum improvement in both thermal and mechanical properties when compared to the neat system. The dispersion of nanoparticles and morphological changes were studied by field emission scanning electron microscopy (FE-SEM) and high resolution transmission electron microscopy (TEM). These results demonstrate that the nanoparticles are spherical in shape (≈30 nm sizes) and are uniformly dispersed over the entire volume of the resin.

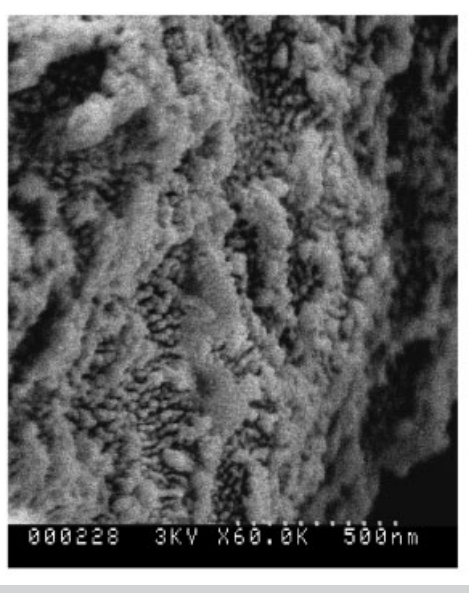

FE-SEM micrograph of the plasma etched 1 wt.-% SiC-epoxy system.

Infusion of SiC Nanoparticles Into SC-15 Epoxy: An Investigation of Thermal and Mechanical Response

Reneé M. Rodgers,[1] *Hassan Mahfuz,**[2] *Vijaya K. Rangari,*[1] *Nathaniel Chisholm,*[1] *Shaik Jeelani*[1]

[1] Center for Advanced Materials (T-CAM), Tuskegee University, Tuskegee, Alabama 36088, USA
[2] Department of Ocean Engineering, Florida Atlantic University, Boca Raton, Florida 33431, USA
Fax: +1-(561)-297-3885; E-mail: hmahfuz@oe.fau.edu

Received: August 5, 2004; Revised: February 4, 2005; Accepted: February 4, 2005; DOI: 10.1002/mame.200400202

Keywords: epoxy; mechanical properties; nanocomposites; nanoparticles; thermal properties

Introduction

Epoxy resin has been of significant importance to the engineering community for many years. Components made of the epoxy-based materials have provided outstanding mechanical, thermal, and electrical properties, and ease of processing.[1] The important factors influencing their performance are the molecular architecture, curing conditions and the ratio of the epoxy resin to curing agent(s). Using an additional phase (e.g., inorganic fillers) to strengthen the properties of epoxy resins has become a common practice.[2] The use of these fillers has been proven to improve the material properties of epoxy resins. Building on the fact that the micro-scaled fillers have successfully been synthesized with epoxy resin,[3–6] the nano-scaled fillers are now being considered to produce high performance composite structures with further enhanced properties. Improvements in mechanical, electrical, and chemical properties have resulted in major interests in nanocomposite materials in numerous automotive, aerospace, electronics and biotechnology applications.[7–9]

A significant amount of work has been done on the effects of fillers on mechanical and thermal properties of epoxies. During the last decade, many studies such as the role of dispersion on the toughening of epoxy,[4,10] effects of nanoparticle fillers on the mechanical behavior of epoxies,[2] and the effect of particle-matrix adhesion on the properties of glass filled epoxies have been conducted. These

 DOI: 10.1002/mame.200400202 © 2005 WILEY-VCH Verlag GmbH & Co. KGaA, Weinheim

modified epoxy systems have yielded improved behavior such as cohesive strength[11] and higher fracture toughness.[5] Dispersion of these fillers into the polymer has been repeatedly indicated as a critical issue. In the absence of a uniform dispersion, particles would tend to agglomerate and cause particle-to-particle rather than the intended particle-to-polymer interaction and eventually result in the degradation of properties.[12–14]

The mechanical and thermal properties of polymers are generally improved by the addition of inorganic additives. The challenges in this area of high performance organic-inorganic hybrid materials are to obtain significant improvements in the interfacial adhesion between the polymer matrix and the reinforcing material since the organic matrix is relatively incompatible with the inorganic phase. Generally, a stronger interfacial bonding will impart better properties to a polymer composite such as high modulus, strength, and hardness as well as resistance to tear, fatigue, cracking, and corrosion.

The present study seeks to investigate the effect of SiC nanoparticles infused into a room temperature cure SC-15 epoxy resin. A similar study[15] performed earlier on epoxy nanocomposites reinforced with carbon fibers has indicated that there is an optimum loading of nanoparticle in the matrix to derive maximum benefit in terms of strength and stiffness of the fibrous composite. In this study, the fiber component has been removed to have an in-depth look at the particle polymer interaction as to how those interactions influence the thermal and mechanical properties of the resulting nanocomposites.

Experimental Part

Synthesis of Nanocomposites

The resin used in this study was a commercially available SC-15 epoxy obtained from Applied Poleramic, Inc. It is a low viscosity two-phased toughened epoxy resin system consisting of part A (resin: mixture of diglycidyl ether of bisphenol-A and aliphatic diglycidyl ether epoxy toughener) and part B (hardener: mixture of cycloaliphatic amine and polyoxyl-alkylamine). The filler β-Silicon carbide (β-SiC) nanoparticles are spherical in shape and are approximately 30 nm in diameter. These nanoparticles were procured from MTI Corporation, Inc. (2700 Rydin Road, Unit D, Richmond, CA, 94804, USA). The dispersion of nanoparticles in resin was carried out with a high intensity ultrasonic liquid processor (Ti-horn, 20 kHz Sonics Vibra Cell, Sonics Mandmaterials, Inc., USA).

The manufacturing of nanocomposites began with the dispersion of β-SiC nanoparticles in part A of SC-15 resin. It is to be noted that the mix ratio of part A and part B of SC-15 is 10:3. The nanoparticles were dispersed in part A since this part is less reactive to ultrasound irradiation than part B. Pre-calculated amount of nanoparticles and part A were carefully weighed, and mixed together in a suitable beaker. This mixing was carried out through a high intensity ultrasonic irradiation for half an hour. In order to avoid a temperature rise during the sonication process, external cooling was employed by submerging the beaker containing the mixture in an ice bath. Once the irradiation was completed, part B was added to the modified part A. The mixing was carried out using a high speed mechanical stirrer for about 10 min. The rigorous mixing of part A and part B produced highly reactive volatile vapor bubbles at the initial stage of the reaction, which if not removed could detrimentally affect the properties of the final product by creating voids.[16] A high vacuum was accordingly applied using a Brand Tech Vacuum system for about 15 min. When the bubbles were completely removed, the mixture was transferred into Teflon-coated metal rectangular molds and kept for 24 h at room temperature. The cured material was then de-molded and trimmed. Finally, test coupons were machined for thermal and mechanical characterization. For comparison, a control panel was also made using neat epoxy (part A and B only, without nanoparticle infusion). In the present study, several wt.-% loadings of nanoparticles were infused with the resin to identify an optimal loading giving the best thermal and mechanical properties. All as-prepared panels were post-cured at 94 °C for 4 h, in a Lindberg/BlueM mechanical convection oven.

Test Procedure

Modulated differential scanning calorimetry (MDSC) and thermogravimetric analysis (TGA) (TA Instruments, Inc., USA) were performed on all the categories of the samples. These experiments were carried out under nitrogen gas atmosphere and the sample sizes were ≈10–25 mg. MDSC were run at a modulation of +/− 1.00 °C every 60 s at a ramp rate of 3.00–200 °C/min. The heating rate for TGA was 10 °C/min. The real time characteristic curves were generated by Universal Analysis 2000-TA Instruments, Inc. data acquisition system. The morphological studies were carried out using field emission scanning electron microscopy (FE-SEM, Hitachi S-900) and scanning transmission electron microscopy (STEM) with electron energy loss spectroscopy (JEOL-2010 STEM-EELS). The FE-SEM samples were precisely cut with a diamond blade, and the polymer was etched by using argon plasma (TEK Vac Industries, Inc. plasma CVD system) with about 600 mTorr argon pressure and 2.5 W/cm^2 intensity for 1 h. The STEM samples were micro-tomed to approximately 200 nm and placed on a copper grid for analysis.

Flexural tests under three-point bend configuration were performed according to ASTM D790-86.[16] The specimen dimensions for flexural tests are shown in Figure 1. The tests were conducted in a 100 KN servo hydraulic testing machine (MTS) equipped with Test Ware data acquisition system. The

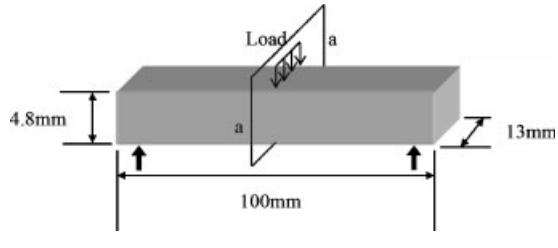

Figure 1. Flexural test coupon (section a-a: plane of fractographical studies).

 © 2005 WILEY-VCH Verlag GmbH & Co. KGaA, Weinheim

machine was run under displacement control mode at a cross-head speed of 1.27 mm/min, and the tests were performed at room temperature. Test coupons were cut from the molded resin using a Felker saw fitted with a diamond-coated steel blade. Five replicate specimens from each category (various wt.-% loadings, and neat) were prepared for static flexure tests.

Results and Discussion

Morphology

Field emission scanning electron microscopy experiments were carried out to understand the shape and sizes of the nanoparticles in the epoxy resin. Figure 2 shows the typical FE-SEM micrograph of the plasma-etched system with 1.0 wt.-% loading. The micrograph clearly indicates that the nanoparticles are well dispersed over the entire volume of the resin. The nanoparticles are seen to be separated and are uniformly embedded in the epoxy resin. The particle sizes are seen to be approximately 30 nm in diameter and are spherical in shape. Agglomeration between particles also appears to be considerably reduced as it was observed earlier with 3 wt.-% loading of SiC[15] nanoparticles. Since the composite surface was plasma etched by argon, the polymer did not get completely removed from the surface, therefore, it was not possible to see the particles alone without the polymer coating around them as seen in Figure 2. It was extremely difficult to differentiate between the particle and polymer patches that were not removed by plasma etching. This called for transmission electron microscopy (TEM) studies which are shown next.

The TEM micrographs shown in Figure 3(a)–(c) confirm that the nanoparticles are indeed well dispersed and there is no observable agglomeration. In addition, the micrograph

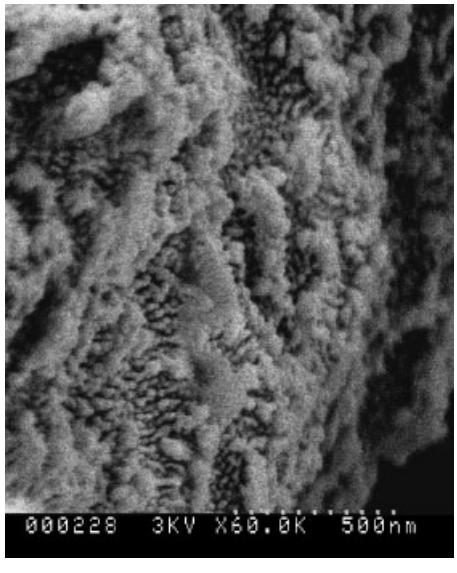

Figure 2. Field emission scanning electron microscopy (FE-SEM) micrograph of the plasma etched 1 wt.-% SiC-epoxy system.

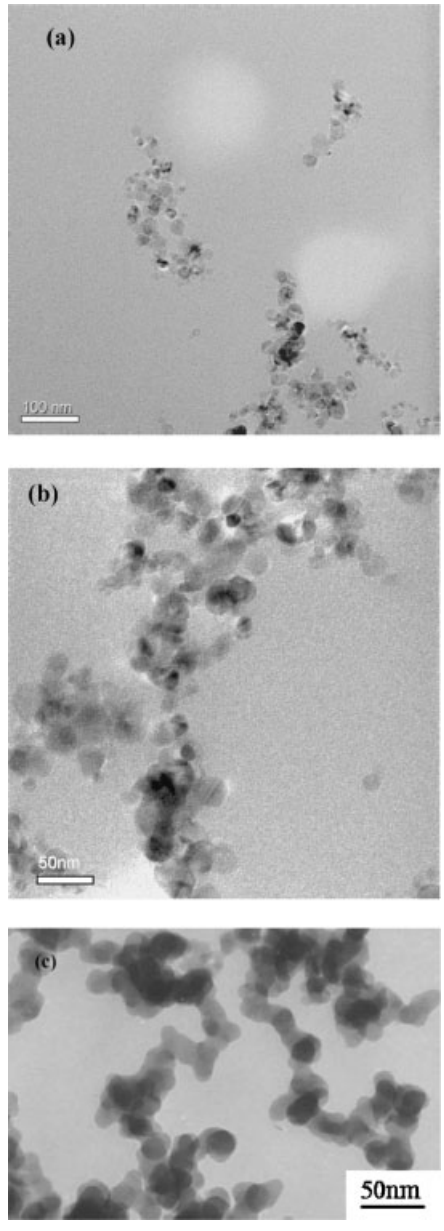

Figure 3. a, b) Transmission electron microscopy (TEM) micrograph of 1 wt.-% SiC-epoxy; c) TEM micrograph of as-received SiC nanoparticles.

of Figure 3(a) shows the presence of the voids along with the nanoparticles. The sizes measured from the micrograph are ≈30 and ≈200 nm for the SiC particles and voids, respectively. Interestingly these voids are always surrounded by the SiC nanoparticles or in some cases the voids are filled with the SiC nanoparticles as shown in Figure 3(b). This suggests that the presence of these nanoparticles inside the void might reduce the void content of the composite, which in turn will improve the mechanical properties. The particle dispersion seen in Figure 3(a) and (b), is not agglomeration although the TEM micrographs give such appearance due to the polymer coating around them. In fact, the dispersion

© 2005 WILEY-VCH Verlag GmbH & Co. KGaA, Weinheim

of particles is very similar to the one received from the manufacturer for the as-produced SiC particles. The TEM micrograph of as-received SiC nanoparticles is shown in Figure 3(c) which looks almost identical to that of Figure 3(b).

Thermal Response

Modulated differential scanning calorimetry analyses were used to measure the changes in heat flow associated with material transition[17] for various wt.-% of SiC nanocomposites. DSC tests were primarily used to determine the effect of SiC nanoparticles on the glass transition temperatures (T_g) of the nanocomposite systems. Typical heat flow versus temperature curves are shown in Figure 4.

Figure 4 shows the DSC curves of four categories of samples. The broad endothermic peak detected in Figure 4(A) at 73 °C is assigned to the T_g of the neat epoxy resin system. The broad endothermic peak is meant to indicate a depression in the curve as seen in Figure 4. The T_g's were determined as the inflection points of the heat flow curves.[18,19] In Figure 4, the T_g's measured for (B) epoxy-0.5 wt.-% SiC, (C) epoxy-1 wt.-% SiC, and (D) epoxy-1.5 wt.-% SiC are 80, 85, and 65 °C, respectively. These results clearly suggest that the T_g has increased by 12 °C from neat epoxy to 1.0 wt.-% SiC system. This increase in T_g is attributed to the increased cross-linking of epoxy resin in the presence of SiC nanoparticles. Usually T_g increases with increasing cross-linking density of epoxy resins because of the restriction in molecular mobility imposed by cross-linking.[20,21] This effect can be understood in terms of decreasing free volume.[22] In the contrary, in Figure 4(D), the T_g of 1.5 wt.-% SiC system has decreased as compared to all other systems including the neat epoxy. The reason for this decrease in T_g could be the agglomeration of SiC nanoparticles. With higher loading, the number of particles is surely high and it becomes more and more difficult to disperse them. Once the particles are agglomerated, the interaction is more between the particles rather than the particle and the polymer. We believe at that stage, the particles begin to act as impurities in the bulk polymer. Also, we believe the volume of the agglomerated particle is much larger and it can no longer occupy the free space. The agglomerated particles can not therefore, impose any restrictions on molecular mobility. On the other hand, the lumped particles can reduce the cross-linking density of the polymer and lower the T_g.

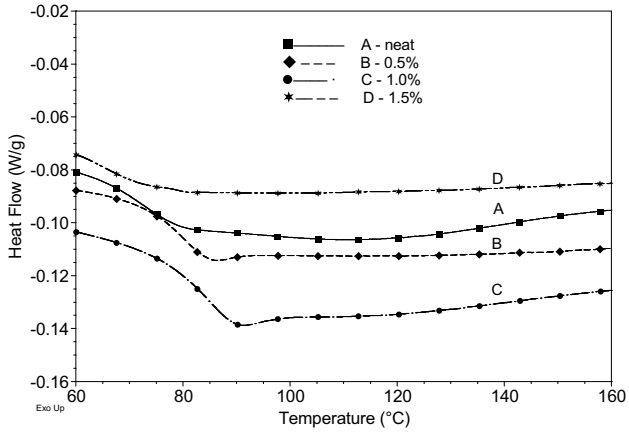

Figure 4. Modulated differential scanning calorimetry (MDSC) curves. A) neat, B) 0.5 wt.-%, C) 1.0 wt.-%, and D) 1.5 wt.-%.

Thermogravimetric analysis measurements were also carried out to obtain information on the thermal stability of the various nanocomposite systems. The TGA data for all the categories of samples are shown in Table 1. In the TGA studies, we can consider either the 50% weight loss or the peak of the derivative curve as a marker for structural decomposition of the samples. Usually, the decomposition of the material begins with 5–10% weight loss of the samples. However, we believe that this weight loss does not signal any structural decomposition in the system. Our experience shows that either the 50% weight loss or the peak of the derivative curve, which in essence indicates the highest rate of weight loss as a function of temperature, is a good approximation to signal the beginning of structural decomposition.[13,23] It is seen in the TGA curves that all samples have only one step degradation, and it is also a common practice to consider the peak degradation temperature as the thermal stability of the system for such cases.[24,25] In our present study, we have considered the derivative peaks as the structural decomposition temperature. As seen in Table 1, the structural decomposition temperatures are 356, 378, and 385 °C for neat, 0.5 and 1.0 wt.-% systems, respectively. If the loading of the SiC particles is increased to 1.5 wt.-%, as shown in Table 1, the decomposition temperature reduces to 358 °C which is very close to that of the neat resin. The reason for no improvement in the decomposition temperature with increased particle loading may be explained macroscopically as a simple colligative thermodynamic effect of an impurity on a bulk solution. Microscopically, it may be seen as the result of the perturbation that the SiC particles introduce into the 3D structure of the polymer. This perturbation weakens the Van der Waals interaction between the polymer chains affecting the stability of the polymer. This perturbation

Table 1. Effects of SiC nanoparticles on differential scanning calorimetry (DSC) and thermogravimetric analysis (TGA).

Material	DSC glass transition temperature (T_g)	T_g increase	TGA decomposition temperature
	°C	%	°C
SC-15 epoxy, neat	73	–	356
+0.5 wt.-% SiC	80	10	378
+1.0 wt.-% SiC	85	16	385
+1.5 wt.-% SiC	65	–	358

 © 2005 WILEY-VCH Verlag GmbH & Co. KGaA, Weinheim

probably begins at a point when the number of particle reaches a certain level and particle-to-particle interaction leads to agglomeration of particles into lumps. We believe the agglomeration of particles begin at around 1.5 wt.-% loading of SiC nanoparticles. It is also noticed that the TGA results are very consistent with those of DSC tests all pointing to the fact that relatively the best thermal performances are achieved with 1 wt.-% system.

Flexural Response

Flexural tests were performed to evaluate the bulk stiffness and strength of each of the nanocomposite systems. Typical stress strain behavior from the flexural tests is shown in Figure 5. The figure shows four curves corresponding to neat, 0.5, 1, and 1.5 wt.-% systems. It is observed in Figure 5 and in Table 2 that the system with 1 wt.-% infusion is relatively the best system with 36% enhancement in modulus and 21% increase in strength. It is also seen from the flexural performance point of view that 0.5 wt.-% system is also very close to the 1.0 wt.-% system having almost identical enhancement in strength and stiffness. However, the mechanical performances begin to degrade with 1.5 wt.-% loading as seen in Table 2. Although the gain in modulus is maintained at this loading, there is hardly any gain in strength.

In a separate study, flexural tests were conducted on the epoxy samples which were only sonicated without any particle infusion. Tests have indicated that the gain in modulus and strength with sonication alone is around 26 and 14%, respectively. This suggests that the gain of 4% in the case of 1.5 wt.-% infusion is actually degradation from the sonicated condition. Effect of an ultrasound in polymer is well known in the literature.[26] Depending on the reaction conditions, ultrasound irradiation can be used for polymerization of monomer without a catalyst by blending the polymers and degrading it to smaller chain lengths. In our case, we believe the improvement in properties is due to the high molecular mixing of part A and formation of reactive free radicals, which helped faster, and efficient cross-linking when part B was added. Most of the contributions came from the sonication alone as evident in Table 2. This happened because the sonication parameters were optimized in our case. For example, if the ultrasound exposure time, amplitude, and surrounding temperature were different, one would get the sonicated polymer properties inferior to that of the unsonicated ones.

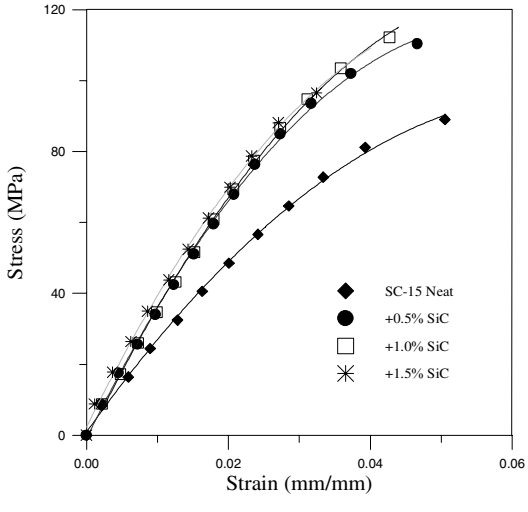

Figure 5. Representative stress versus strain curves from flexural tests.

Enhancement in strength in the range of 21% during flexure was somewhat surprising due to the fact that previous studies with nanoclays[27,28] did not show such improvement. Our understanding is that the nanoclay particles having micron size planar dimensions provide relatively less interaction with the polymer chains even in a fully exfoliated condition. On the other hand, if dispersed properly, spherical nanoparticles of ≈30 nm diameter can sit very comfortably within the polymer chains and coils which have more or less similar dimensions.[6,29] Moreover, if the center of the nanoparticles is close to the radius of gyration of the polymer coils, the number of atoms at the surface will increase significantly. This in turn will enhance the reactivity between the particle and the polymer. More reactivity will translate into increased changes in polymer properties such as cross-linking, rate of cure, and other thermal properties. This is what we have observed with our DSC and TGA results with spherical nanoparticle infusion, and which we see have a direct bearing on the mechanical properties as well.

In an attempt to investigate the fracture behavior of neat and nano-phased SC-15, SEM and optical micrographs were taken and are shown in Figure 6. The fractured surfaces shown in Figure 6 represent the cross-sectional view of the specimen as one would look into either from right or left hand side of the specimen. The top surface of the specimen is under compression and the bottom is under tension. The specimens under investigation were below the loading point. As it is seen in Figure 6(a), the specimens of both categories failed primarily on the tension side as a combination of crumbled matrix and propagation of cracks emanating from material flaws located near the edge of the specimens. Magnified views of the matrix cracks are shown in Figure 6(b). It is noticed in the figure that matrix cracks are more of a ductile nature in neat SC-15 as opposed to a brittle failure in case of nano-phased SC-15. This was expected in the sense that one would make the matrix more brittle by introducing ceramic nanoparticles in it. Also visible is the presence of a dominant failure crack [Figure 6(b)] in the nano-phased specimen which is however not present in the neat specimen. If we now follow the crack propagation from the material flaws, as shown in

© 2005 WILEY-VCH Verlag GmbH & Co. KGaA, Weinheim

Table 2. Flexural test data.

Material	Flexural modulus	Gain/loss in modulus	Flexural strength	Gain/loss in strength
	GPa	%	MPa	%
SC-15 epoxy, neat (unsonicated)	2.45 ± 0.09		91.87 ± 5.13	
SC-15 epoxy, neat (sonicated)	3.09 ± 0.10	26.12	104.79 ± 6.65	14.06
0.5 wt.-% SiC/SC-15	3.26 ± 0.21	33.06	111.73 ± 9.35	21.62
1.0 wt.-% SiC/SC-15	3.33 ± 0.21	35.92	111.53 ± 6.97	21.40
1.5 wt.-% SiC/SC-15	3.32 ± 0.10	35.51	95.86 ± 4.01	4.34

Figure 6(c), we find that the cracks spread out in radial manner in both cases, but coalesced into a dominant one only in the nano-phased sample, again indicating a brittle nature of failure modes. The conclusion therefore, from the SEM and optical studies is that due to nanoparticle infusion, the failure modes of SC-15 epoxy basically shifted from a relatively ductile to a brittle one.

Conclusion

A summary of the above investigations is given in the following:

- Ultrasonic cavitation has been shown to be an efficient method of infusing silicone carbide nanoparticles into the SC-15 epoxy resin.

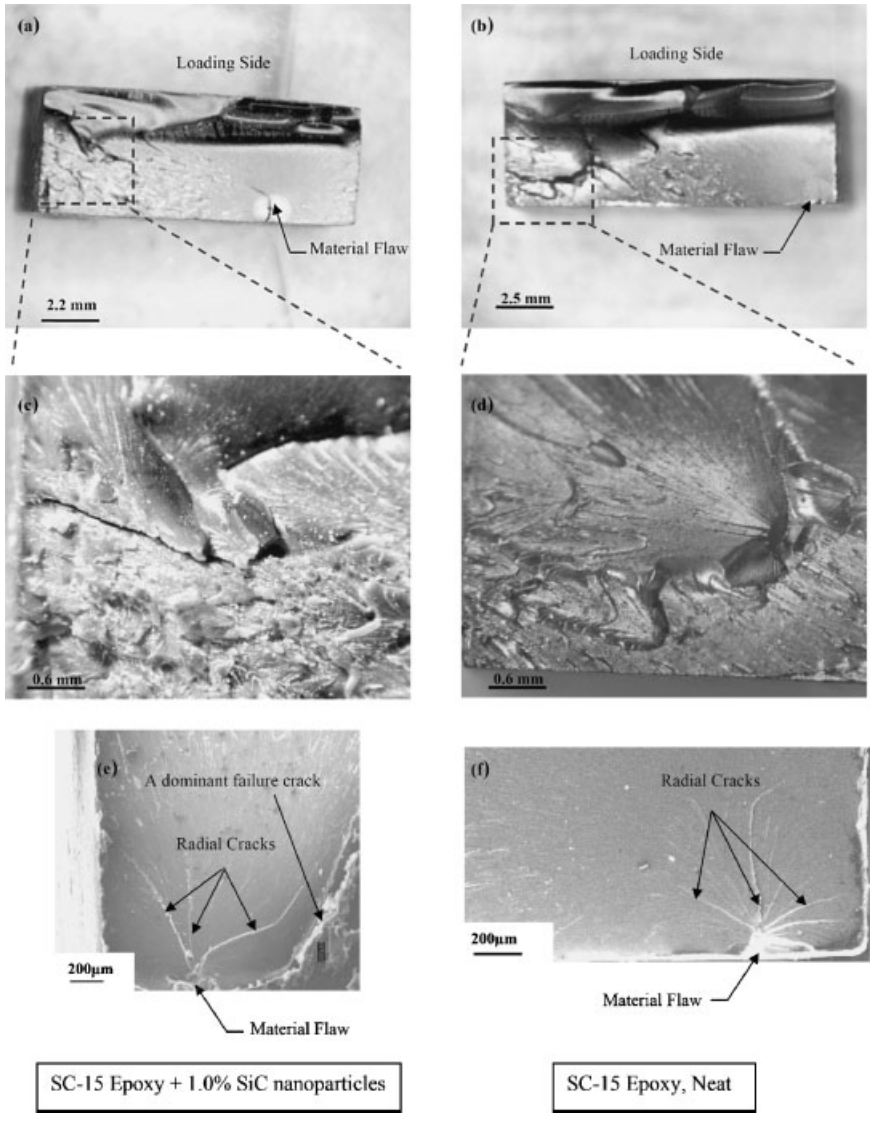

Figure 6. Optical and SEM micrographs of fractured surfaces. a, c, e) SC-15 epoxy + 1.0% SiC nanoparticles; b, d, f) SC-15 epoxy, neat.

 © 2005 WILEY-VCH Verlag GmbH & Co. KGaA, Weinheim

- Sono-chemical reaction enhances polymer properties, and also disperses nanoparticles uniformly over the entire volume of the resin.
- Optimal loading of the SiC nanoparticles is seen to be around 1 wt.-% for the best combination of thermal and mechanical properties of the nanocomposites. Nanoparticle loading beyond this point (1 wt.-%) seems to degrade properties and it becomes severe around 2 wt.-% loading.
- There has been consistent improvement in thermal and mechanical properties of nanocomposites with 1 wt.-% SiC infusion over their neat counterparts. For example, the structural decomposition temperature and T_g increased by 29 °C and 16%, respectively. In case of mechanical properties, flexural stiffness and strength improved by 21–36% range.
- It was also noticed that with 1 wt.-% loading the resin maintained sufficient viscosity which would make it suitable for future processing of fibrous composites through vacuum assisted resin transfer molding (VARTM).

Acknowledgements: The authors would like to thank the *Office of Naval Research* (ONR) and the *National Science Foundation* (NSF) for supporting this work.

[1] J. B. Donnet, *Compos. Sci. Technol.* **2003**, *63*, 1085.
[2] Y. Zheng, Y. Zheng, R. Ning, *Mater. Lett.* **2003**, *57*, 2940.
[3] R. J. Day, P. A. Lovell, A. A. Wazzan, *Compos. Sci. Technol.* **2001**, *61*, 41.
[4] R. Bagheri, R. A. Pearson, *Polymer* **2000**, *41*, 269.
[5] T. Kawaguchi, R. A. Pearson, *Polymer* **2003**, *44*, 4239.
[6] H. Mahfuz, A. Adnan, V. K. Rangari, S. Jeelani, B. Z. Jang, *Compos. Part A: Appl. Sci. Manuf.* **2004**, *35*, 519.
[7] V. M. F. Evora, A. Shukla, *Mater. Sci. Eng.* **2003**, *A361*, 358.
[8] M. Hussain, Y. Oku, A. Nakahira, K. Niihara, *Mater. Lett.* **1996**, *26*, 177.
[9] D. Schmidt, D. Shah, E. Giannelis, *Curr. Opin. Solid State Mater. Sci.* **2002**, *6*, 205.
[10] J. Y. Qian, R. A. Pearson, V. L. Dimonie, O. L. Shaffer, M. S. El-Aasser, *Polymer* **1997**, *38*, 21.
[11] T. Kawaguchi, R. A. Pearson, *Polymer* **2003**, *44*, 4229.
[12] H. Mahfuz, N. Chisholm, A. Ashfaq, V. Rangari, S. Jeelani, "*BSME-ASME Conference*", Keynote lecture, January 2004.
[13] H. Mahfuz, M. S. Islam, V. K. Rangari, M. C. Saha, S. Jeelani, *Compos. Part B: Eng.* **2004**, *35*, 543.
[14] H. Mahfuz, V. K. Rangari, M. S. Islalm, S. Jeelani, *Compos. Part A: Appl. Sci. Manuf.* **2004**, *35*, 453.
[15] N. Chisholm, H. Mahfuz, V. Rangari, A. Ashfaq, S. Jeelani, *Compos. Struct.* **2005**, *67*, 115.
[16] A. S. D790-86, in: *ASTM Standard* D790-86, 1986.
[17] B. Wetzel, F. Haupert, M. Q. Zhang, *Compos. Sci. Technol.* **2003**, *63*, 2055.
[18] A. G. Loera, F. Cara, M. Dumon, J. P. Pascault, *Macromolecules* **2002**, *35*, 6291.
[19] R. Vijaya, Y. Koltypin, Y. S. Cohen, D. Aurbach, O. Palchik, I. Felner, A. Gedanken, *J. Mater. Chem.* **2000**, *10*, 1125.
[20] W. D. Cook, M. Mehrabi, G. H. Edward, *Polymer* **1999**, *40*, 1209.
[21] S. Monstserrat, *J. Polym. Sci., Part B: Polym. Phys.* **1994**, *32*, 509.
[22] S. Monstserrat, *Polymer* **1995**, *36*, 435.
[23] S. Ganguli, D. Dean, K. Jordan, G. Price, R. Vaia, *Polymer* **2003**, *44*, 6901.
[24] P. Shuwen, A. Yuxian, B. F. Chengchen, Z. Yugang, D. Lisong, *Polym. Degrad. Stabil.* **2003**, *80*, 141.
[25] P. Cardiano, P. Mineo, S. Sergi, R. C. Ponterio, M. Triscare, P. Piraino, *Polymer* **2003**, *44*, 4435.
[26] K. S. Suslick, G. J. Price, *Annu. Rev. Mater. Sci.* **1999**. *29*, 295.
[27] S. C. Jana, S. Jain, *Polymer* **2001**, *42*, 6897.
[28] C. B. Ng, L. S. Schadler, R. W. Siegel, *Nanostruct. Mater.* **1999**, *12*, 507.
[29] R. J. Young, P. A. Lovell, "*Introduction to Polymers*", 2nd edition, Nelson Thornes Ltd., Cheltenham, UK 2002.

© 2005 WILEY-VCH Verlag GmbH & Co. KGaA, Weinheim